Science of the Total Environment 737 (2020) 140209

Contents lists available at ScienceDirect

Science of the Total Environment

journal homepage: www.elsevier.com/locate/scitotenv

Optimization of an MMPB Lemieux Oxidation method for the quantitative analysis of microcystins in fish tissue by LC-QTOF MS

Maryam Tabatabaei Anaraki [a], René S. Shahmohamadloo [b], Paul K. Sibley [b], Karen MacPherson [c], Satyendra P. Bhavsar [a,c], André J. Simpson [a], Xavier Ortiz Almirall [c,d,*]

[a] Department of Physical and Environment Sciences, University of Toronto Scarborough, Toronto, ON, Canada
[b] School of Environmental Sciences, University of Guelph, Guelph, ON, Canada
[c] Ontario Ministry of the Environment, Conservation, and Parks, Toronto, ON, Canada
[d] School of Environmental Sciences, Queen's University, Kingston, ON, Canada

HIGHLIGHTS

- A method for microcystins analysis in fish was optimized by factorial design.
- Use of matrix matched calibration *in-situ* generated MMPB for improved accuracy.
- Validation included a 96-h exposure test, where toxins accumulated in the liver.
- Low concentration of microcystins were detected in sixteen rainbow trout fillets.
- High concentration of microcystins were detected in ten rainbow trout livers.

GRAPHICAL ABSTRACT

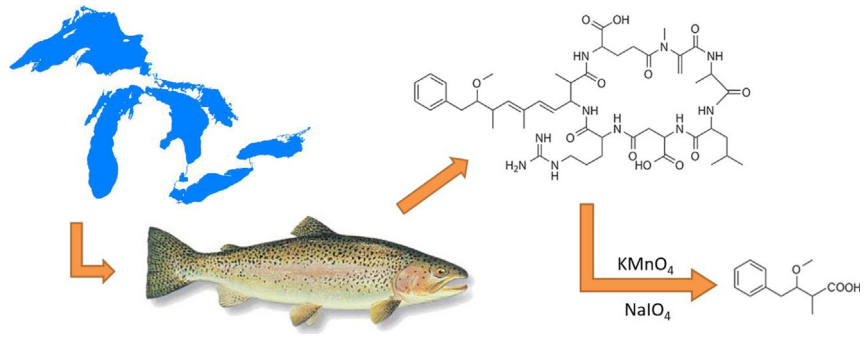

ARTICLE INFO

Article history:
Received 8 April 2020
Received in revised form 11 June 2020
Accepted 12 June 2020
Available online 15 June 2020

Editor: Yolanda Picó

Keywords:
Cyanobacteria
Microcystin
MMPB
Fractional factorial design
In-situ standard generation
Matrix matched calibration curve

ABSTRACT

Microcystins are toxic heptapeptides produced by cyanobacteria in marine and freshwater environments. In biological samples such as fish, microcystins can be found in the free form or covalently bound to protein phosphatases type I and II. Total microcystins in fish have been quantified in the past using the Lemieux Oxidation approach, where all toxins are oxidated to a common fragment (2-methyl-3-methoxy-4-phenylbutyric acid, MMPB) regardless of their initial amino acid configuration or form (free or protein bound). These studies have been carried out using different experimental conditions and employed different quantification strategies. The present study has further investigated the oxidation step using a systematic approach, to identify the most important factors leading to a higher, more robust MMPB generation yield from fish tissue in order to reduce the method detection limit. Field samples were quantified using an *in-situ* generated MMPB matrix matched calibration curve by isotope dilution with d_3-MMPB *via* liquid chromatography coupled to time-of-flight mass spectrometry (LC-QTOF MS). This approach improves method's accuracy by taking into account of potential matrix effects that could affect the derivatization, sample prepation and instrumental analysis steps. The validated method showed 16.7% precision (RSD) and +6.7% accuracy (bias), with calculated method detection limits of 7.28 ng g^{-1} Performance of the method was assessed with the analysis of laboratory exposed Rainbow Trout (*Oncorhynchus mykiss*) to cyanobacteria as a positive control, where no microcystins were detected in the pre-exposure fish liver and fillet, low levels in the exposed fillet (65.0 ng g^{-1}) and higher levels in the exposed

* Corresponding author at: Ontario Ministry of the Environment, Conservation, and Parks, Toronto, ON, Canada.
E-mail address: xavier.ortiz@ontario.ca (X. Ortiz Almirall).

https://doi.org/10.1016/j.scitotenv.2020.140209

liver (696 ng g^{-1}). Finally, the method was employed for the analysis of 26 fillets (muscle) and livers of Walleye (*Sander vitreus*) and Yellow Perch (*Perca flavescens*) from Lake Erie, showing very low concentrations of microcystins in the fillet and higher concentrations in liver, up to 3720 ng g^{-1}.

1. Introduction

Microcystins are potent hepatotoxins produced by freshwater cyanobacteria including *Anabaena*, *Chroococcus*, *Microcystis*, *Nostoc*, *Oscillatoria*, and *Planktothrix* (Christoffersen and Kaas, 2000). It has been well-documented that microcystins inhibit serine/threonine protein phosphatases 1 and 2A in the liver of humans and animals, causing cytoskeletal damage, breakdown of hepatocytes, pooling of blood followed by hemorrhaging and organ failure (Christoffersen and Kaas, 2000). These toxins can also cause reproductive and gastrointestinal toxicity, and affect the immune system of different species (Chen et al., 2016; Kubickova et al., 2019; McLellan and Manderville, 2017; Svirčev et al., 2019). Microcystins have been the causes of sickness and death in humans, mammals, fish, birds, mussels, and zooplankton, and continue to threaten freshwater ecosystems (Gene et al., 2019; Huisman et al., 2018; Shahmohamadloo et al., 2019b; Shahmohamadloo et al., 2020).

Microcystins have a cyclic heptapeptide structure, comprising different amino acids; however, all known congeners contain an uncommon β-amino acid, with a 3-amino-9-methoxy-2,6,8-trimethyl-10-phenyldeca-4(E),6(*E*)-dienoic acid structure (Rinehart et al., 1988), generally known as Adda. The different amino acid substitutions in the microcystin cyclic peptide structure can lead to thousands of theoretical configurations, among which approximately 250 have been identified and reported to date (Martens, 2017; Bouaïcha et al., 2019). Although the Adda amino acid can present different substitutions in the methoxy group (acetylation or hydrogen substitution), the methoxylated moiety is found in about 80% of the known variants, as well as the most commonly observed microcystins in cyanobacterial blooms worldwide, such as microcystin-LR (Bouaïcha et al., 2019). Although microcystins are found in the unbound, free-form inside the cyanobacterial cells or dissolved in water (also known as intra- and extracellular microcystins, respectively), studies reveal that they can bioaccumulate into animal tissues (Humbert, 2009) where they exist as both free and covalently-bound to protein phosphatases type 1 and 2 (Robinson et al., 1991). The World Health Organization has set 0.04 μg kg^{-1} body weight per day as the tolerable daily intake guideline value for microcystin-LR, the most commonly detected variant (WHO, 2008).

Various analytical techniques have been applied to determine the presence and concentration of microcystins in fish tissue. Enzyme linked immunosorbent assay -ELISA- (Metcalf et al., 2000; Nagata et al., 1995) and protein phosphatase inhibition assay -PPIA- (Ward et al., 1997) are cost-effective approaches for the analysis of microcystins in tissue that allow the integration of all microcystin variants in a sample. However, studies have demonstrated that this approach might be prone to false positive detections of microcystins due to matrix effects interfering with the test (Geis-Asteggiante et al., 2011; Lawrence and Menard, 2001; Moreno et al., 2011). Extraction of free microcystin fractions combined with liquid chromatography-mass spectrometry (LC-MS) based techniques is one of the most common procedures to test for microcystins in fish tissue. These methods follow microcystin extraction procedures using several solvents that mostly target free microcystins (Mekebri et al., 2009; Schmidt et al., 2013). Unlike the previously mentioned bioassays, LC-MS differentiates between microcystin congeners, though it limits users to the determination of congeners that are not covalently bound to proteins and for which standards are available.

An alternative approach for the analysis of total microcystins —including all variants, in free and protein-bound forms— is the Lemieux Oxidation method. The Lemieux Oxidation reaction was originally explored by Lemieux and Rudolff in 1955 (Lemiuex and Rudloff, 1955) for the oxidation of olefins by sodium metaperiodate, in the presence of potassium permanganate as a catalyst. Regardless of its original structure, oxidizing every microcystin congener under Lemieux condition will produce the following common fragment from the Adda [(2*S*, 3*S*, 8*S*, 9*S*)-3-amino-9- methoxy-2, 6, 8-trimethyl-10-phenyldeca-4E, 6E-dienoic acid] amino acid: 2-methyl-3-methoxy-4-phenylbutyric acid (MMPB). Several laboratories have successfully employed this approach for the analysis of total microcystins in complex matrices such as harmful algal blooms or fish tissue (Mohamed et al., 2019; Roy-Lachapelle et al., 2015; Duncan et al., 2018; Flores et al., 2018; Bieczynski et al., 2013; Cadel-Six et al., 2014; Foss et al., 2017; Foss and Aubel, 2015; Greer et al., 2017, 2018; Neffling et al., 2010; Ott and Carmichael, 2006; Roy-Lachapelle et al., 2014; Suchy and Berry, 2012; Vudathala et al., 2017; Wu et al., 2009); however, experimental conditions between studies varied substantially. Table 1 summarizes recent studies that have used the Lemieux Oxidation method to analyze microcystins, including a comparison between experimental conditions. As it can be observed in the table, there is little consistency between the amount of sample used (from 10 to 1000 mg), oxidation time (from 1 to 4 h), potassium permanganate concentration (2 to 500 mM) or even choice of internal standard (if any), just to name a few experimental conditions.

Considering differences in the experimental conditions and quantification strategies presented thus far in the literature, here we optimize an LC-MS-based determination of total microcystins in fish tissue (*e.g.*, liver, muscle) using a Lemieux Oxidation method through an experimental design, paired with an *in-situ* generation of matrix-matched calibration standards. A fractional factorial design was applied to the Lemieux Oxidation method to investigate how different experimental factors can affect the MMPB oxidation. Furthermore, an *in-situ* matrix-matched calibration curve was generated by oxidation of four microcystin standards spiked to blank *Oncorhynchus mykiss* liver and muscle tissue to account for matrix effects and correct for the yield of MMPB generation. Ultra-performance liquid chromatography-quadrupole/time-of-flight mass spectrometry (LC-QTOF-MS) in tandem mode (MS/MS) was employed in the present study to achieve detection limits of microcystin as low as 7.28 ng g^{-1} of dried *Oncorhynchus mykiss* tissue.

2. Experimental

2.1. Standards and reagents

All microcystin standards (-LR, -YR, -RR, and -LA) were purchased from Enzo Life Sciences (Farmingdale, NY, USA). Potassium carbonate, potassium permanganate, sodium metaperiodate, sodium bisulfite, sulfuric acid, methanol, and formic acid (FA) were purchased from Fischer Scientific (Markham, Canada). Solvents used in this study were LC-MS grade. A standard of MMPB (2-methyl-3-methoxy-4-phenylbutyric acid) and its deuterated form, d_3-MMPB (internal standard), were purchased from Wako Chemicals (Richmond, VA, USA). Waters Oasis HLB 3 cc (400 mg) LP extraction cartridges were purchased from Waters (Milford, MA, USA). Water (18.2 MΩcm, organic carbon content ≤8 μg l^{-1}) was obtained from a Millipore Milli-Q A10 (Etobicoke, ON, Canada) station.

2.2. Microcystis aeruginosa culture preparation

Microcystis aeruginosa strain CPCC 300 was acquired from the Canadian Phycological Culture Centre (University of Waterloo, Waterloo, Canada). Growth of this strain was unicellular, and the diameter of

Table 1
Review of Lemieux oxidation conditions for the determination of microcystins in fish reported in the recent and relevant publications.

References	Matrix	Quantification strategy	Internal standard	Sample amount (g)	Oxidation time (hr)	[KMnO4] (M)	[NaIO3] (M)	pH	Method detection limits	Instrumental analysis
(Mohamed et al., 2019)	Fish muscles	External calibration curve	N/A	0.01 dried tissue	3	0.1	0.1	9	N/A	LC-MS
(Duncan et al., 2018)	Algae	MMPB-*d3* dilution calibration	d_3-MMPB	0.02 dried	1	0.2	0.5	9	1 μg L^{-1}	LC- MS/MS
(Brown et al., 2018)	Dolphin liver	Matrix spikes and matrix standard curve	No IS	0.01 dried	2.5	0.1	0.1	N/A	1.3 μg g^{-1}	LC–MS/MS
(Flores et al., 2018)	Fish liver and muscle	N/A	N/A	N/A	N/A	N/A	N/A	N/A	N/A	GC–MS
(Greer et al., 2018)	Pig liver	Matrix matched calibration curve, MMPB spiked after pH adjustment	No IS	0.05 dried	2	0.2	0.2	N/A	N/A	UPLC-MS/MS
(Foss et al., 2017)	Periphyton, Fish liver and whole juvenile	*In situ* matrix matched calibration curve	No IS	dried	2	0.25	0.25	N/A	2 ng g^{-1} periphyton 3 ng g^{-1} liver and whole juvenile	LC-MS/MS
(Greer et al., 2017)	Fish muscle	Matrix matched calibration curve, MMPB spiked after pH adjustment	No IS/Nodularin	0.05 dried	2	0.1	0.1	N/A	N/A	UPLC-MS/MS
(Vudathala et al., 2017)	Fish liver and plasma	*In situ* matrix matched calibration curve	No IS	0.5 liver wet 0.4 g plasma	3	0.2	0.2	≥9	6.2 ng g^{-1} liver 5.2 ng g^{-1} plasma	LC-MS/MS
(Foss and Aubel, 2015)	Water	*In situ* matrix matched calibration curve	4-PB	N/A	0.5	0.15	0.15	N/A	0.05 μg L^{-1}	LC-MS/MS
(Roy-Lachapelle et al., 2015)	Fish muscles and whole	Matrix matched calibration curve, MMPB spiked before SPE	4-PB	1 wet	2	0.5	0.5	9	2.7 ng g^{-1}	LDTD-APCI-MS/MS
(Cadel-Six et al., 2014)	Fish liver, intestines, gills, and muscles	MMPB standard calibration curve	No IS	0.06 dried intestinal tissue 0.01 dried liver, gills, and muscles	4	0.1	0.1	9	1.5 ng mL^{-1}	LC-MS/MS
(Roy-Lachapelle et al., 2014)	Water	Internal calibration	4-PB	N/A	1	0.5	0.5	9	0.2 μg L^{-1}	LDTD-APCI-MS/MS
(Bieczynski et al., 2013)	Fish intestine and liver	MMPB generated by MC-LR oxidation	No IS	1 wet	overnight	0.002	0.09	9	0.2 ng g^{-1}	GC–MS
(Suchy and Berry, 2012)	Fish liver and muscle	Me-MMPB calibration curve	4-PB	1 mL of (7 g homogenized in 5 mL water)	3	0.36	0.096	9	40 ng g^{-1}	SPME-GC/MS
(Neffling et al., 2010)	Snail tissue and serum	N/A	N/A	0.01 dried tissue Serum: 1 mL	3	0.1	0.1	9	N/A	LC-MS/MS
(Wu et al., 2009)	Cyanobacteria	MMPB standard calibration curve	No IS	0.05 dried	1–4	0.5	0.2	9	1 ng g^{-1}	HPLC
(Ott and Carmichael, 2006)	Liver	*In situ* matrix matched calibration curve	4-PB	1 wet	3	0.02	0.02	9	5 ng g^{-1}	LC-MS

cells ranged between 1 and 2 μm. *M. aeruginosa* CPCC 300 produces two microcystin congeners, microcystin-LR and [D-Asp^3]-microcystin-LR. *M. aeruginosa* CPCC 300 cultures were prepared according to Shahmohamadloo et al. (2019a). Briefly, cultures were maintained in BG-11 medium under continuous light (600 ± 15 lx cool-white fluorescent light) with a specified temperature (24.0 ± 1 °C) for 16: 8 h of light: dark cycle in a growth chamber. Cultures were grown for at least 1 month prior to cell lysis for use in the experiment. Prior to running our study, we investigated whether BG-11 medium could result in lethal or growth impairment in the test organism, *O. mykiss*. Results confirmed that *O. mykiss* did not experience lethality or growth impairment from exposure to BG-11 medium.

M. aeruginosa cultures were pooled into one vessel with a final cell density of 1.88×10^7 cell ml^{-1}. Water samples were collected for chemical analysis at the Toxic Organics Section of the Ministry of the Environment, Conservation and Parks in Etobicoke, Canada, following the protocol of Ortiz et al. (2017). Results confirmed that *M. aeruginosa* produced 446 μg l^{-1} of total microcystins (24.8 fg $cell^{-1}$), which was comprised of 296 μg l^{-1} microcystin-LR (16.5 fg $cell^{-1}$) and 150 μg l^{-1} [D-Asp^3]-microcystin-LR (8.34 fg $cell^{-1}$). *M. aeruginosa* were lysed by a 3 × freeze-thaw cycle in order to prepare extracellular microcystins, as described in Ortiz et al., 2017.

2.3. Method validation experiments with Oncorhynchus mykiss

2.3.1. Lemieux Oxidation optimization using fractional factorial design

Factorial designs are widely used in experimental investigations and screening portion of experiments (Boddy and Smith, 2011; Ortiz et al., 2011; Plackett and Burman, 2006). Fractional factorial designs enable users to eliminate some redundant experimental conditions and hence the number of experiments. Factorial design experiments allow studying a given number of factors (*e.g.*, experimental condition such as time and temperature) at two different levels (*e.g.*, 1 h *vs* 2 h). Factorial design of limited set of variables with two levels has advantage over

the conventional methods which vary single parameters per trial. The fractional factorial design results enable to define the variables, their levels of contribution, and their optimal ranges to gain the maximum information possible with running the minimum number of experiments. Furthermore, factorial experiment allows to study the effect of each factor separately and in interactions with other factors. For the optimization of the Lemieux Oxidation method in this study, seven factors at two levels were investigated. Applying fractional factorial design enabled us to reduce the number of treatment combinations from 128 to 8 experiments.

In this study, the the Lemiuex Oxidation of microcystins to MMPB detection was optimized using a saturated fractional factorial design. Based on preliminary experiments, seven factors that could influence the oxidation of microcystins were chosen (Table 2A): pH, concentration of potassium permanganate and sodium metaperiodate, oxidation duration, fish tissue, fish tissue amount, and initial volume of oxidation solution. Table 2B illustrates the oxidation conditions of the experimental design, allowing to study seven factors at two different levels with only 8 treatment combinations.

2.3.2. Laboratory exposed fish validation test

A 96-hour method validation test was conducted on *O. mykiss* (130 g average size) exposed to extracellular microcystins produced by *M. aeruginosa* CPCC 300. The test was comprised of a water-only control and a single extracellular microcystins treatment (89.2 μg l^{-1} of total microcystins). Each treatment had 4 replicates of 20 L pails with three *O. mykiss* per replicate, totalling 24 fish for the test. Water parameters (*i.e.*, temperature, pH, conductivity, dissolved oxygen, and total ammonia) were measured at 0 h and 96 h. Water samples were collected at 0 h and 96 h to measure the total of MCs at the beginning and end of the test. Liver and muscle tissue were individually collected from all *O. mykiss* at 96 h and frozen at −80 °C until analysis by the Lemieux Oxidation method.

2.3.3. Environmental samples

The number of reported algal blooms in Lake Erie has been increasing steadily the last few years (Carmichael and Boyer, 2016), posing a potential drinking water thread affecting over 11 milion people (Wituszynski et al., 2017). The validated analytical method was used to analyze several Walleye (*Sander vitreus*) and Yellow Perch (*Perca flavescens*) samples, as these fish species are the most commonly harvested sport and commercial fish in Lake Erie. The samples were collected from Lake Erie during fall of 2015, and stored at −80 °C until analysis. These samples were analyzed to validate the performance of the Lemieux Oxidation method with real fish liver and muscle environmental samples. The total number of *O. mykiss* samples analyzed were 10 liver and 18 muscle tissues, which were not paired.

2.4. Sample preparation

Approximately 500 mg of liver and muscle tissue from each sample was homogenized, and frozen at −80 °C. Frozen tissues were freeze-dried using a Labcono Freezone 2.5 freeze-drier from Fischer Scientific, (Markham, ON, Canada) for a minimum of 24 h, after which samples were ground to a fine powder using a pestle and mortar. Freeze-dried samples were individually stored in labelled vials at −40 °C until analysis. Fish sample (100 mg of freeze-dried liver or fillet) spiked with internal standard (d_3-MMPB), were oxidized at pH 8.5 using potassium permanganate (0.3 mM) and sodium periodate (20 mM) for two hours. More detailed information about how these experimental parameters were optimized can be found in the *Results and Discussion* section.

Excess of oxidizing solution was quenched with sodium bisulphite and pH adjusted to 3 with 10% sulfuric acid. Oasis HLB 3 cc (400 mg) LP extraction cartridges were used for extraction and clean-up of MMPB and d_3-MMPB. Catridges were initially conditioned with 10 mL of methanol and 10 mLof 0.1% FA milli-Q water. Sample was then loaded and washed with 10 mL of 0.1% FA milli-Q water and 10 mL of 50% methanol. Analytes were eluted with 4 mL of methanol. Collected samples from the elution step were dried down to 250 μL using a gentle nitrogen stream at 35 °C, and then diluted to 1 mL using 0.1% FA milli-Q water. Samples were filtered prior to instrumental analysis using Pall GHP filters (Mississauga, ON, Canada).

2.5. Quality assurance and quality control

For each batch of 20 processed samples, a blank fish sample (freeze-dried *O. mykiss* liver/muscle raised in the laboratory under controlled conditions, spiked with d_3-MMPB) and a spiked fish sample (500 ng g^{-1} of total microcystins) were included. No detectable levels of microcystins were expected to be found in the blank, whereas concentration determined in the spiked sample was expected to be within ±30% of 500 ng g^{-1}.

Table 2
A. Selected factors and their levels for factorial design, with best conditions in bold.
B. Experimental design matrix.

A

Selected factors	Level (-)	Level (+)
Potassium permanganate (mM)	20	**0.3**
Sodium metaperiodate (mM)	**20**	5
pH	7.7	**8.5**
Fish amount (mg d.w.)	50	**100**
Fish matrix	**Filet**	**Liver**
Oxidation duration (hr)	3	**2**
Initial volume of oxidation solution (mL)	Low (~5)	**Large (~20)**

B

Run	Potassium permanganate (mM)	Sodium metaperiodate (mM)	pH	Fish amount (g)	Fish matrix	Oxidation duration (h)	Initial volume of oxidation solution (mL)	MMPB conversion (%)
1	20	20	7.7	100	Liver	2	5	21.8
2	0.3	20	7.7	50	Fillet	2	20	26.9
3	20	5	7.7	50	Liver	3	20	7.4
4	0.3	5	7.7	100	Fillet	3	5	19.6
5	20	20	8.5	100	Fillet	3	20	4.4
6	0.3	20	8.5	50	Liver	3	5	23.4
7	20	5	8.5	50	Fillet	2	5	33.3
8	0.3	5	8.5	100	Liver	2	20	25.7

2.6. Chromatography and mass spectroscopy conditions

For the chromatographic separation, a Waters Acquity I Class Chromatograph by Waters Corporation (Milford, MA, USA) was employed. Two different liquid chromatograph (LC) configurations were investigated for the analysis: conventional LC —limiting the maximum sample amount to be injected to 20 μL—, and on-line solid phase extraction mode (Ortiz et al., 2017) where up to 500 μL can be injected and trapped prior to the gradient LC separation.

For the conventional LC experiments, mobile phases used were 0.1% formic acid in water (mobile phase A) and 0.1% formic acid in methanol (mobile phase B), at a constant flow of 0.35 mL min^{-1}. The gradient program started at 95% mobile phase A during the first 3.75 min (isocratic), linearly ramping to 95% mobile phase B at minute 12.25, and held until 14 min. The system was set back to its initial conditions during the last 2 min, for a total chromatographic run time of 16 min. The chromatographic column used was a Waters BEH C18, 50 × 2.1 mm, 1.7 μm particle size by Waters Corporation (Milford, MA, USA).

For the on-line SPE experiments, the trapping stage was carried out with a secondary binary pump, where mobile phases used were 0.1% formic acid in water (mobile phase C) and 0.3% formic acid in a 2:1 methanol-water mixture (mobile phase D) at 2 mL min^{-1}. The mobile phase was set to 100% C during the first 3.5 min (trapping stage), then 95% D until 6 min (to rinse the trapping column), and then back to initial conditions until 12 min. The chromatographic column used for the trapping stage was a Waters XBridge C8, 30 × 2.1 mm, 10 μm particle size by Waters Corporation (Milford, MA, USA). For the gradient separation stage, conditions were the same as described for conventional LC.

A quadrupole time-of-flight-mass spectrometer (QTOF-MS) was employed for the detection of the compounds. MMPB showed better sensitivity in positive mode during full scan analysis (MS), whereas negative mode had better sensitivity for the MRM transition (MS/MS). For this reason, the instrument was operated in positive mode for MS acquisition and negative for MS/MS acquisition modes, at 2.5 kV capillary voltage, 40 V sampling cone, 125 °C source temperature and cone gas (nitrogen) at 50 L h^{-1}. During the method development stage, two acquisition modes where compared: high resolution (25,000), high mass accuracy (< 2 ppm) full scan mode, and tandem mass spectrometry (MS/MS) mode for the 207.1027 → 131.0874 transition at 10 eV collision energy (210.1210 → 131.0874 for the d_3-MMPB internal standard). Although not monitored in the present study, tansitions 193.0870 → 131.0874 and 235.0976 → 131.0874 can additionally be included to accoult for the less common desmethylated and acetylated

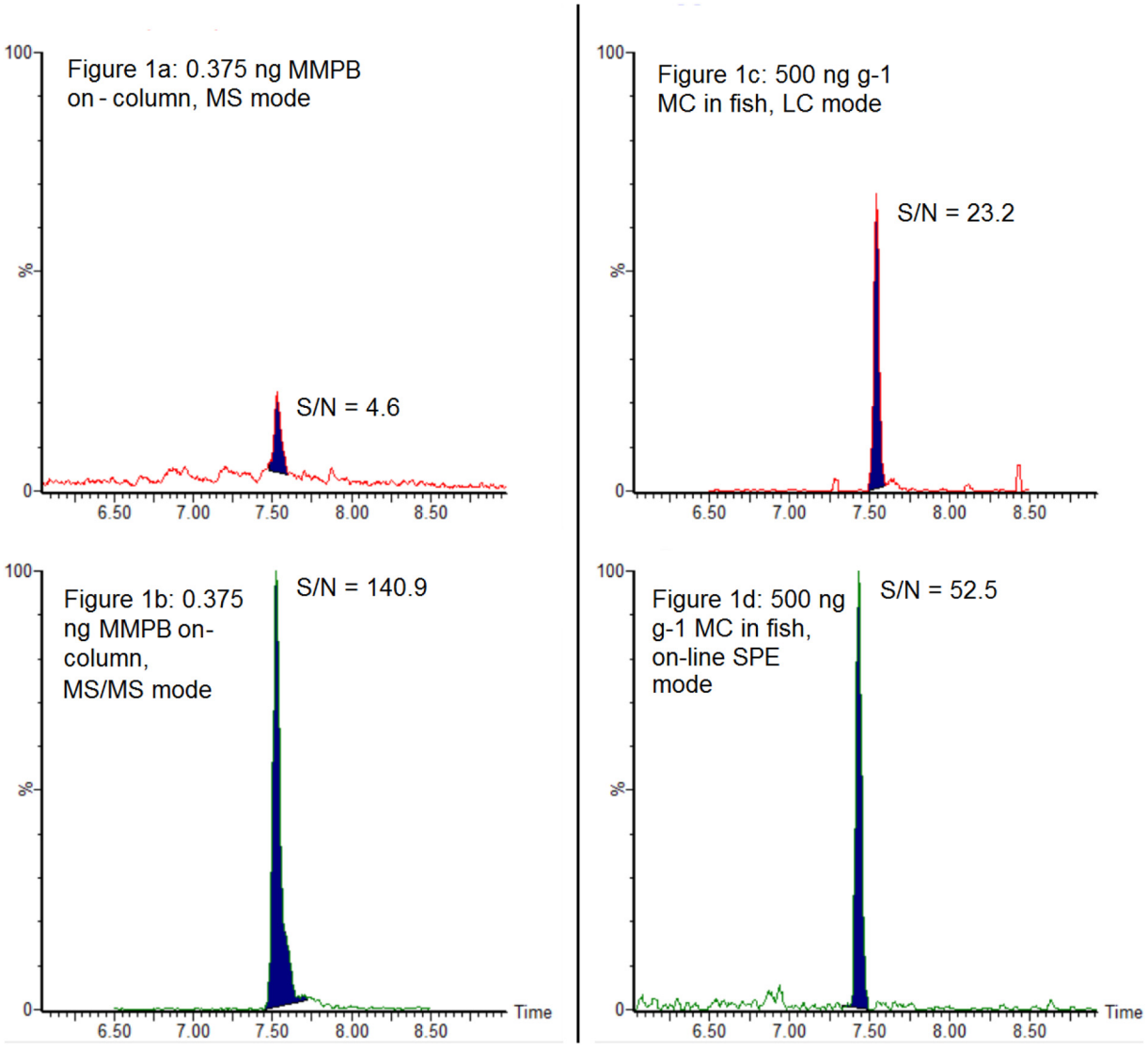

Fig. 1. LC-QTOF MS instrumental analysis optimization, showing MMPB signal-to-noise ratio for: 0.375 ng MMPB on-column standard injection in negative MS (1a) and negative MS/MS (1b) modes, and *in-situ* generated MMPB from 500 ng g^{-1} of microcystins in fish (fillet) in conventional LC (1c) and on-line SPE (1d) modes by negative MS/MS.

Adda substitutions, respectively. For the full scan MS and MS/MS experiments, the target enhancement feature of the selected ion was enabled to increase the sensitivity of the target compounds.

3. Results and discussion

3.1. LC-QTOF chromatographic and mass spectrometric optimization

Prior to the optimization of the microcystin oxidation conditions, instrumental conditions for the detection of MMPB had to be determined. The present study was carried out using a QTOF-MS, a versatile instrument that can acquire data in different modes. In full scan MS mode, selectivity towards measurement of the target compound is enhanced by measuring its *m/z* with high resolution and high mass accuracy, being able to distinguish the exact mass of the analyte from other interfering isobaric compounds with nominal mass. Alternatively, in MS/MS mode selectivity for targeted compounds is increased by monitoring a specific precursor to product ion transitions. For this reason, the best MS acquisition method for MMPB analysis was investigated prior to optimizing the LC conditions, by injecting 15 μL of a 25 ng mL^{-1} MMPB standard solution (0.375 ng on column). MMPB showed very poor ionization efficiency in positive mode, about nine times less than negative mode. Fig. 1 illustrates the results for the analysis of MMPB in negative mode full scan MS (Fig. 1a, m/z = 207.1027) and negative mode MS/MS (Fig. 1b, m/z = 131.0874 fragment), with collision energy manually optimized at 10 eV. As evident in this figure, sensitivity was substantially increased (about 3.5×) when switching from negative MS to MS/MS mode. MS data also showed some interferences around 7.8 min that were not observed with MS/MS due to its higher selectivity. For this reason, MS/MS in negative mode was selected for the analysis of MMPB.

Conventional LC methods typically inject 5 to 20 μl of sample, to avoid problems such as ion suppression or chromatographic peak broadening. Larger amounts of sample can be injected when instruments are configured for on-line SPE, with an extra pump and trapping column. In brief, up to several mL of sample are injected and trapped in the first column, cleaning up the sample from the most polar-interfering compounds. Using a six-port valve, analytes are desorbed in reverse flow by a secondary pump, and separated in time by gradient chromatography (Ortiz et al., 2017; Fayad et al., 2015). This principle can also be used for injecting equivalent amounts of analyte in the instrument while reducing the need to evaporate under a stream of nitrogen, which is regarded as one of the most time consuming steps of sample preparation.

There are two key parameters that should be optimized for on-line SPE coupled to LC, injection volume and solvent composition. If the injection volume is too low it will not increase the method's sensitivity enough. If injection volume is too large tagteted analytes could not be focused efficiently, breaking through the trapping column. It could also lead to ion suppression matrix effects if the volume injected is not properly washed. As for the injection solvent, higher contents of water could lead to solubility problems of organic compounds, whereas higher contents of organic solvent (*e.g.* methanol) could prevent the analytes for being trapped in reverse phase chromatography. Fig. 2 shows the on-line SPE optimization results using injection volumes from 50 to 500 μl of sample (0.5 ng μl^{-1} MMPB), in mixtures of water:methanol ranging from 0 to 100% organic content.

As it can be obserbed, very poor trapping efficiency was obtained using 100% methanol, as MMPB would not be retained in the reverse phase trapping column. Results slightly increased using 75% methanol, but trapping efficiency plateaued when larger volumes of samples were injected (300–500 μl). Mixtures containing 25 and 0% methanol showed similar results, with much better retention. Best results were obtained with 50% methanol mixtures, with no substantial signal improvement between 400 and 500 μl injected volumes. For this reason, the optimized on-line SPE conditions for MMPB analysis were injecting 400 μl of sample in a 50:50 water:methanol mixture.

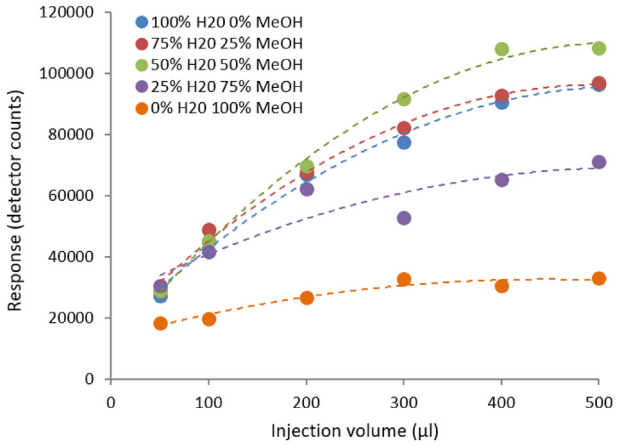

Fig. 2. On-line SPE injection volume and solvent composition optimization.

In order to compare the LC and on-line SPE approaches, two different sample preparation workflows were carried out using *in-situ* generated MMPB from spiking the fish fillets at 500 ng g^{-1}: injecting 15 μl from a 300 μl extract in conventional LC mode (Fig. 1c) and 400 μL from a 1000 μl extract in on-line SPE mode (Fig. 1d). Signal-to-noise (calculated as peak to peak) doubled from 23.2 to 52.5 when using the on-line SPE configuration. For this reason, combined with the fact that it also entails less sample pre-concentration, the on-line SPE chromatographic configuration was preferred. This technique also offers an extra clean-up step, reducing matrix effects of complex samples. Nevertheless, the increase in sensitivity is only a factor of two compared to conventional LC, which means that comparable method performance could be obtained by using conventional LC when the on-line SPE is not available.

3.2. Lemieux Oxidation factorial design results

Generally, the Lemieux Oxidation method of freeze-dried fish tissues for microcystin determination begins by the addition of oxidant solution to the sample, previously spiked with internal standard (Table 1). The oxidant solution contains potassium permanganate and sodium metaperiodate in alkaline condition ranging from pH 7 to 10 (Lemieux and Rudloff, 1955). More oxidation solution is added if the colour of sample solution turns from purple to yellow/brown until the colour turns to purple again, to make sure the oxidizing agent is not the limiting reagent. Based on previous studies (Table 1), the duration of the oxidation step is carried out within two or three hours at room temperature. The reaction is quenched by adding sodium bisulphite until the sample is colourless, and 10% sulfuric acid solution is added until the pH of the solutions becomes acidic (~2) prior to the SPE clean-up stage.

Previous studies by Lemieux and Rudloff show that pH, potassium permanganate, and sodium metaperiodate concentrations affect the oxidation yield (Table 1). Therefore, these were chosen in two levels in the factorial design experiment. Moreover, the primary target organ of microcystin toxicity is the liver (Falconer, 1991). However, studies show that organic anion-transporting polypeptides, which mediate the transportation of microcystins to the liver, are also expressed in other organs such as the stomach (Žegura et al., 2011). Bearing in mind that muscle tissue is most commonly consumed by humans, liver and muscle tissue in two different amounts (50 and 100 mg) were chosen as the fish matrix and fish amount factors, respectively. The length of oxidation (2 and 3 h) and initial volume of oxidation solution (5 mL and 20 mL) were chosen as two additional factors.

Blank fish tissues were spiked with microcystin-LR, -RR, -YR and -LA (125 ng g^{-1} each, 500 ng g^{-1} total). Eight runs incorporating a combination of the seven factors (Table 2B) were conducted. Mass labelled

d_3-MMPB was used throughout the experimental design as an internal standard, spiked before the oxidation step at 500 ng g^{-1}. As it can be observed in the table, MMPB conversion yields were heavily influenced by the experimental conditions, with recoveries ranging from 4.4% (experiment 5) to 33.3% (experiment 7). Although it is difficult to identify which factors influenced these recoveries due to the number of experimental parameters changed between each experiment, the results suggest that lowest recoveries (experiments 3 and 5) were carried out during 3 h of oxidation, whereas the highest recoveries (experiments 1, 2, 7, 8) were carried out during 2 h.

The effect of modifying these different factors on the generation of MMPB can be more accurately quantified and visualized by calculating the effect (%) of each selected factor (Eq. (1)). This effect represents how the measured output (MMPB generation) increased or decreased moving from levels (-) to (+), in %.

$$\text{Effect}\ (\%) = \frac{(\text{Average result level}+) - (\text{Average result level}-)}{\text{Average result (levels + and}-)} \times 100 \quad (1)$$

Calculation of the effect (%) from a selected factor in an experimental design.

As Fig. 3 illustrates, with the exception of pH, the various factors exhibited similar effects on MMPB and d_3-MMPB recovery. The factorial design demonstrates that when going from lower pH (7.7) to higher pH (8.5), the MMPB generation will have 30% higher recovery while this is opposite to the internal standard that leads to decrease in its recovery to <50%. As discussed earlier, moving from 3 to 2 h of oxidation duration gave better results of about 30 and 40%, for d_3-MMPB and MMPB, respectively. The factorial design results also indicated little difference between the two fish tissues used (liver or muscle) and a10–15% negative effect on d_3-MMPB and MMPB when a lower amount of fish tissue (50 mg) was used compared to higher amount (100 mg). Potassium permanganate at lower concentration (0.3 mM) indicated about 25% and 10% positive effects on MMPB and d_3-MMPB recovery, respectively. The concentration of sodium metaperiodate had litte effect on MMPB yield, for this reason the highest concentration is preferred (20 mM) to ensure that the oxidizing agent is still in excess by the end of the reaction. A larger initial volume of oxidant solution (~20 mL) gave ~10% better recovery for both *d3*-MMPB and MMPB compared to 5 mL. In most cases, samples starting with5 mL oxidizing volumehad to be topped up to 20 mL after half an hour.

The Lemieux Oxidation method optimized factors obtained from factional factorial design is shown in Table 2. Factorial design revealed pH and oxidation duration are the two most important factors that affect the oxidation yield. While oxidation duration of 2 h is best for both d_3-MMPB and MMPB, pH has the opposite effect. This means that higher pH will not only oxidize the Adda amino acid and generate more MMPB but also oxidize d_3-MMPB from the start of the experiment. To compromise generation of MMPB and oxidation of d_3-MMPB the optimized pH was set to 8.0 for the Lemieux Oxidation method. Moreover, factorial design indicated a negative effect of 10–15% on d_3-MMPB and MMPB using high amount of fish tissue (100 mg). However, to increase the limit of detection and since the effect is negligible, 100 mg of freeze-dried fish tissue was set for the optimized oxidation process.

3.3. Oxidation duration

To further study the effect of oxidation duration on MMPB generation and d_3-MMPB degradation, oxidation of microcystins in fish tissue at different time points (from 0 to 4 h) was carried out applying the optimized Lemieux Oxidation conditions (Table 2A), which covers the range of oxidation duration previously reported in literature (Table 1). As illustrated in Fig. 4, generation of the MMPB fragment from microcystins steadily increases over the first 2 h of oxidation to reach a maximum yield of 30% of molar conversion. After this, the generated MMPB is further oxidized to other degradation products. Also, d_3-MMPB concentration decreases over time since it was spiked at 0 h, recovering about 78% of the initial concentration after 2 h and 34% after 4 h of oxidation. Thus, the results indicate that 2 h of oxidation may be the best compromise between MMPB generation from microcystins and d_3-MMPB internal standard recovery.

3.4. Calibration curve by in-situ generation of MMPB calibration standard

As Table 1 shows, different strategies have been previously used to quantify microcystins in fish. Approaches that directly use MMPB standard for quantification might not take into account the variability of

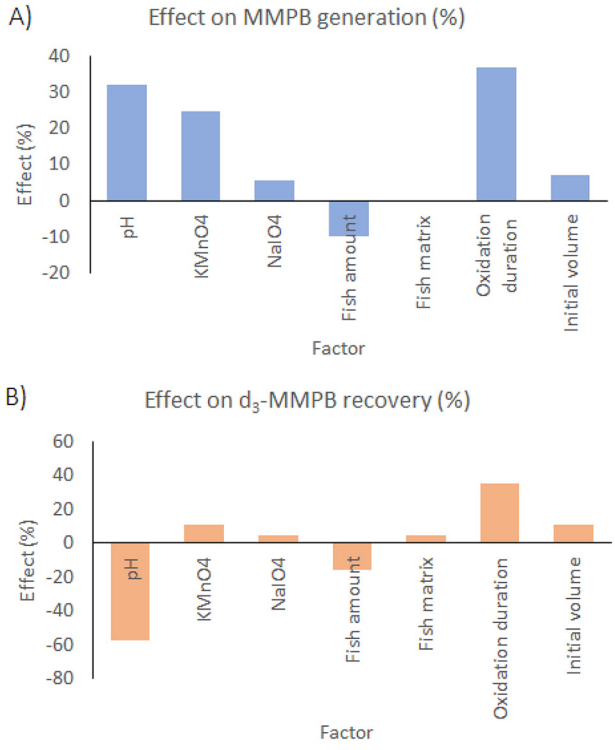

Fig. 3. Effects of studied factors on MMPB generation (A) and d_3-MMPB recovery (B).

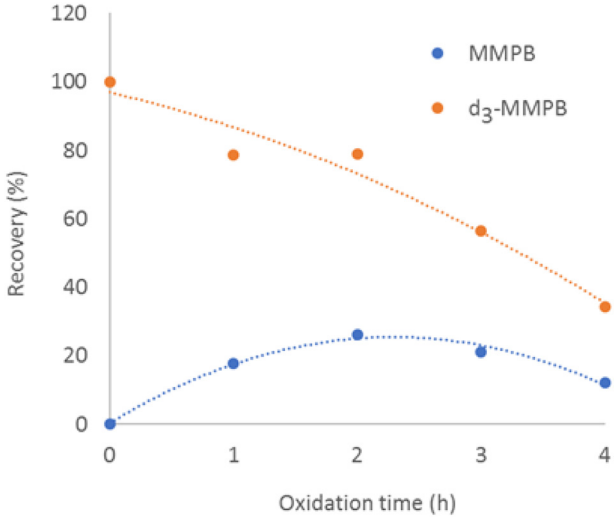

Fig. 4. MMPB and d_3-MMPB generation/decomposition curve at different oxidation duration time points.

MMPB generation from microcystins in the presence of fish tissue. Like any other analytical method, the choice of internal standard addition and in what step of sample preparation the standard is added might also affect the final results. In order to minimize the potential bias of these fators, the present method employs for the first time (to our knowledge) spiked microcystin-LR, -YR, -RR and -LA to *in situ* generate the MMPB calibration curve in fish filet or liver, to account for variability during the oxidation stage and matrix effects. Furthermore, the method is improved by the use of d_3-MMPB internal standard, to account for variable ionization efficiency at the exact retention time of the target analyte during the LC-MS analysis. In order to do so, fish tissues (100 mg of freeze-dried fillet or liver) were spiked with a fixed amount of d_3-MMPB (500 ng g^{-1}) and a mixture of microcystins LR, LA, RR, YR to give total concentrations ranging from 5 to 2000 ng g^{-1}. Four different variants were used instead of only one to better represent the different conversion yields that individual microcystins might have. For quantification purposes and yield recovery calculations using microcystins and MMPB standards, it should be taken into account that the mass conversion rate from microcystins to MMPB is approximately 5 to 1 (*e.g.*, microcystin-LR has a molar mass of 995.2 Da and generates one MMPB fragment of 208.2 Da), which means that a 5 ng g^{-1} microcystin standard is equivalent to a 1 ng g^{-1} MMPB *in-situ* generated standard.

Fig. 5 shows an example of an *in-situ* MMPB generated matrix matched calibration curve using d_3-MMPB as an internal standard (orange curve), including 11 calibration levels (0, 5, 10, 25, 50, 125, 250, 500, 750, 1000 and 2000 ng microcystin g^{-1}). The method shows very good linearity ($R^2 = 0.9956$) considering that the target analyte is generated *in-situ* over a dynamic range of almost three orders of magnitude, with all residuals within +/− 30% from the linear regression. In order to highlight the importance of how different quantification strategies can affect the final results, a calibration curve using an MMPB standard (not generated from microcystins) and d_3-MMPB as internal standard, added at the same molar ratio as the matrix matched curve, is also represented in Fig. 5 (blue). As mentioned previously, after 2 h of oxidation the recovery of d_3-MMPB (78.9%) is higher than the generated MMPB (30.0%), thus leading to a lower relative response (MMPB/d_3-MMPB) than the calibration curve using the standards. The *in-situ* generated MMPB curve slope is three times lower than the one using the MMPB standards, which means that the latter one is underestimating the real concentration by a factor of 3. Using one of the Lake Erie samples detailed in the Section 2.3.2 as an example, a sample containing 3720 ng g^{-1} of microcystins (Liver sample #1) calculated using the *in-situ* generated curve would only have quantified 1213 ng g^{-1} if a curve using MMPB standards had been used instead, being biased low as it doesn't take into account the different analyte and internal standard recovery ratio obtained during the oxidation stage. Very similar results would be obtained for samples quantified with an external calibration curve (no internal standard correction), using *in-situ* generated MMPB from oxidized microcystins (≈30% conversion yield) or an MMPB standard, where the latter approach would be underestimating the final concentration by a factor of 3.3, as it would not take into account the actual MMPB conversion yield in real samples.

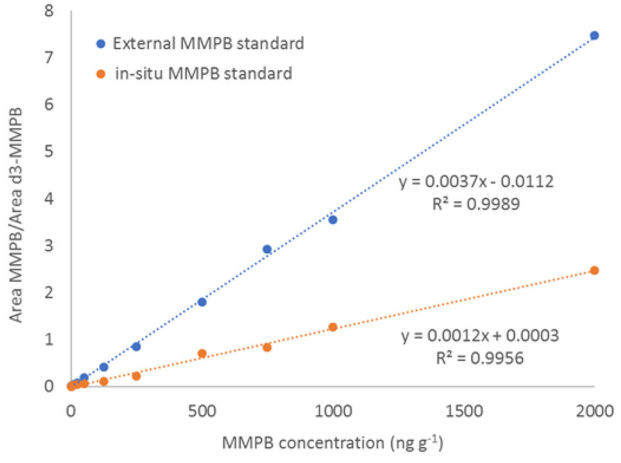

Fig. 5. Calibration curves using *in-situ* generated MMPB and external MMPB standard.

The *in-situ* generated MMPB matrix matched quantification method was validated by analyzing twelve blank samples spiked at 250 ng microcystins g^{-1}, including two different fish tissues (fillet and liver) analyzed by two different analysts (3 fillets and 3 liver samples each). Precision was determined within 16.7% RSD, with an accuracy bias of +6.7% of the target value. The method showed good linearity between 10 and 2000 ng g^{-1}, with R2 > 0.995 and individual residuals within 30% from the curve. Method detection limit (calculated as three times the standard deviation at 10 ng g^{-1} spiked sample analyzed five times) was 7.28 ng g^{-1}, and method quantification limit (ten times the standard deviation) was 24.3 ng g^{-1}.

3.5. Determination of microcystins in liver and muscle tissue from 96-hour exposure test

To evaluate the performance of the validated method, a fish exposure test was carried out to obtain real (not spiked) fish tissue containing microcystins. Ten *O. mykiss* were exposed for 96 h to a lysed culture of *M. aeruginosa* that produced a concentration of 89.2 μg l^{-1} of total microcystins (59.3 μg l^{-1} of microcystin-LR and 29.9 μg l^{-1} of [D-Asp^3]-microcystin-LR), analyzed as per Ortiz et al. (2017). No proteins were removed from the lysed extract.Ten other *O. mykiss* were kept in the same conditions in water-only, as controls. Liver and muscle tissue from exposed and control fish were analyzed separately with the optimized method. As shown in Table 3, no microcystins were detected in the control liver or muscle tissues. For exposed fish, microcystins were

Table 3
MC-LR concentration determination results in the laboratory exposed and control fish (*O. mykiss*, $N = 10$).

Liver	MCs (ng g^{-1})	Fillet	MCs (ng g^{-1})	Liver to filet accumulation ratio
Blank spiked at 500 ng g^{-1}	503.3	Blank spiked at 500 ng g^{-1}	518.8	–
Blank	<LOD	Blank	<LOD	–
Control 1	<LOD	Control 1	<LOD	–
Control 2	<LOD	Control 2	<LOD	–
Control 3	<LOD	Control 3	<LOD	–
Control 4	<LOD	Control 4	<LOD	–
Control 5	<LOD	Control 5	<LOD	–
Control 6	<LOD	Control 6	<LOD	–
Control 7	<LOD	Control 7	<LOD	–
Control 8	<LOD	Control 8	<LOD	–
Control 9	<LOD	Control 9	<LOD	–
Control 10	<LOD	Control 10	<LOD	–
Exposed1	1355	Exposed 1	121	11.2
Exposed2	553	Exposed 2	63	8.8
Exposed3	780	Exposed 3	75	10.4
Exposed4	724	Exposed 4	64	11.3
Exposed5	424	Exposed 5	21	20.2
Exposed6	482	Exposed 6	42	11.5
Exposed7	944	Exposed 7	104	9.1
Exposed8	804	Exposed 8	39	20.6
Exposed9	425	Exposed 9	70	6.1
Exposed10	463	Exposed 10	53	8.7
Avg.	696	Avg.	65	11.8
RSD %	42	RSD%	46	41

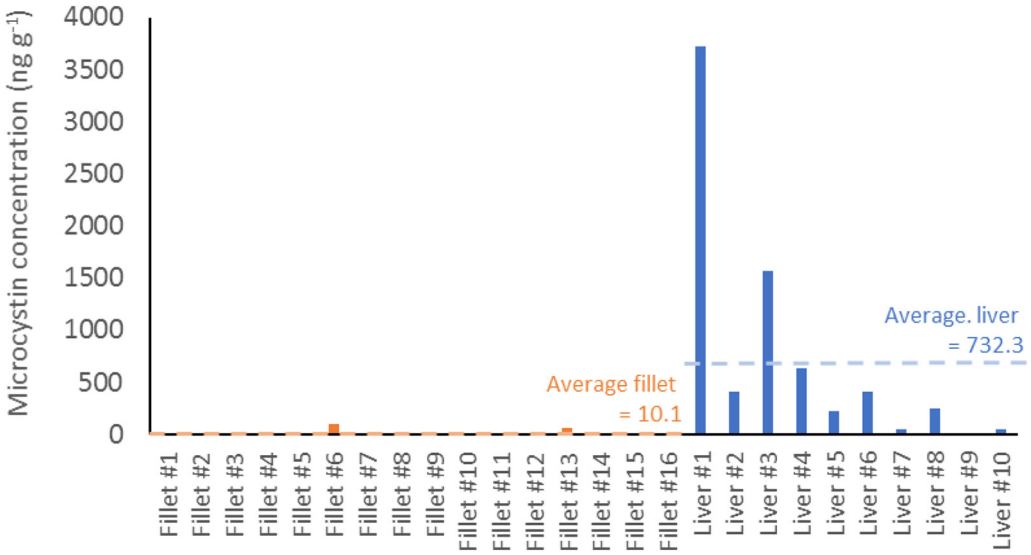

Fig. 6. Microcystin concentrations determined in Walleye and Yellow Perch collected from Lake Erie. (For interpretation of the references to colour in this figure legend, the reader is referred to the web version of this article.)

detected in all the analyzed muscles at an average concentration of 65 ng g^{-1}, whereas concentrations in liver tissue were much higher at an average concentration of 696 ng g^{-1}. Although the relative standard deviation between replicates was near 40%, likely reflecting biological variability due to the different sizes of each fish, the accumulation ratio between liver and muscle remained fairly constant, evidencing an accumulation of microcystins in the liver about 11 times higher than in muscle tissue. This observation is in agreement with the wide body of literature evidencing that the liver is a key target organ for the accumulation of microcystins which could lead to hepatotoxicity (Falconer, 1991). From a human risk assessment perspective, the significantly lower concentraitons in muscle tissue is encouraging since fish muscle is usually the only part used for consumption, whereas liver and other offal are usually discarded.

3.6. Determination of MCs in environmental samples

Tissue samples from twenty-six Walleye and Yellow Perch (16 fillet and 10 liver) samples from Lake Erie were analyzed with the validated method (Fig. 6). Unlike the exposure study described in Section 3.6, in this case fillets and livers were not paired. Microcystins were only detected in two of the sixteen fillets analyzed, at concentrations of 61.3 and 99.6 ng g^{-1}, with an average microcystin concentration in fillet of 10.1 ng g^{-1} (averaging the 2 samples avobe and the 14 samples below detection limits). Much higher levels were determined in the livers, where microcystins were detected in nine out of the ten samples processed. Values ranged from 52.1 to 3720 ng g^{-1}, with an average microcystin concentration in liver of 732 ng g^{-1}.

4. Conclusion

A method for the analysis of microcystins in fish by Lemieux Oxidation was optimized using a saturated fractional factorial design. Among the seven parameters studied, pH and oxidation time were determined as the most critical factors for the generation of MMPB. When the oxidation is carried out for 2 h, adjusting the pH to 8.5, with 20 mL of potassium permanganate and sodium metaperiodate concentrations of 0.3 and 20 mM respectively, using 100 mg of freeze-dried sample (liver or muscle indistinctly), MMPB generation yield from microcytsins in the presence of matrix was around 30%. To the knowledge of the authors, this is the first study to optimize the MMPB conversion using a relatively large amount of sample (100 mg d.w.) and two different tissues (fillet/liver), improving the method's robustness for matrix effects and sample representativity. Moreover, in order to improve the method's accuracy, a multi-level matrix matched calibration standard curve with *in-situ* MMPB generation was used for the quantification of total microcystins in fish, using d_3-MMPB as the internal standard. The analysis method was validated showing a 16.7% precision (RSD) and +6.7% accuracy (bias), with calculated method detection limits of 7.28 ng g^{-1}. The method validation was completed by analyzing a set of samples from Rainbow Trout fish exposed to *M. aeruginosa* in a laboratory; no toxins were detected in control livers and muscles, low levels of microcystins were detected in muscle (average concentration of 65.0 ng g^{-1}), and much higher levels detected in liver (696 ng g^{-1}). Total 26 liver and fillet samples of Walleye and Yellow Perch from Lake Erie were analyzed with the validated method, showing very low microcystin levels in fillets (average concentration of 10.1 ng g^{-1}) and much higher concentrations in livers (average concentration of 732.3 ng g^{-1}, with a sample as high as 3719.7 ng g^{-1}). To our knowledge, this is the first time a method for the analysis of microcystins in fish is validated with a real positive control (not spiked), evidencing that fish can accumulate over 10 times more microcystins in liver than muscle tissue.

CRediT authorship contribution statement

Maryam Tabatabaei Anaraki: Methodology, Investigation, Validation, Formal analysis, Writing - original draft. **René S. Shahmohamadloo:**Methodology, Investigation, Writing - review & editing.**Paul K. Sibley:**Investigation, Resources, Writing - review & editing.**Karen MacPherson:**Investigation, Resources, Writing - review & editing.**Satyendra P. Bhavsar:**Investigation, Resources, Funding acquisition, Writing - review & editing.**André J. Simpson:** Investigation, Resources, Funding acquisition, Writing - review & editing.**Xavier Ortiz Almirall:**Conceptualization, Methodology, Resources, Investigation, Supervision, Writing - review & editing, Project administration.

Declaration of competing interest

The authors do not have any conflict of interest to declare.

References

Bieczynski, F., Bianchi, V.A., Luquet, C.M., 2013. Accumulation and biochemical effects of microcystin-LR on the Patagonian pejerrey (Odontesthes hatcheri) fed with the toxic cyanobacteria Microcystis aeruginosa. Fish Physiol. Biochem. https://doi.org/10.1007/s10695-013-9785-7.

Boddy, R., Smith, G., 2011. Central composite designs. Effective Experimentation. https://doi.org/10.1002/9780470666654.ch12.

Bouaïcha, N., Miles, C.O., Beach, D.G., Labidi, Z., Djabiri, A., Benayache, N.Y., Nguyen-Quang, T., 2019. Structural diversity, characterization and toxicology of microcystins. Toxins https://doi.org/10.3390/toxins11120714.

Brown, A., Foss, A., Miller, M.A., Gibson, Q., 2018. Detection of cyanotoxins (microcystins/nodularins) in livers from estuarine and coastal bottlenose dolphins (Tursiops truncatus) from Northeast Florida. Harmful Algae 76, 22–34. https://doi.org/10.1016/j.hal.2018.04.011.

Cadel-Six, S., Moyenga, D., Magny, S., Trotereau, S., Edery, M., Krys, S., 2014. Detection of free and covalently bound microcystins in different tissues (liver, intestines, gills, and muscles) of rainbow trout (Oncorhynchus mykiss) by liquid chromatography-tandem mass spectrometry: method characterization. Environ. Pollut. https://doi.org/10.1016/j.envpol.2013.10.016.

Carmichael, W.W., Boyer, G.L., 2016. Health impacts from cyanobacteria harmful algae blooms: implications for the North American Great Lakes. Harmful Algae https://doi.org/10.1016/j.hal.2016.02.002.

Chen, L., Chen, J., Zhang, X., Ping, X., 2016. A review of reproductive toxicity of microcystins. J. Hazard. Mater. https://doi.org/10.1016/j.jhazmat.2015.08.041.

Christoffersen, K., Kaas, H., 2000. Toxic cyanobacteria in water. A guide to their public health consequences, monitoring, and management. Limnol. Oceanogr. https://doi.org/10.4319/lo.2000.45.5.1212.

Duncan, K.D., Beach, D.G., Wright, E.J., Barsby, T., Gill, C.G., Krogh, E.T., 2018. Direct online quantitation of 2-methyl-3-methoxy-4-phenyl butanoic acid for total microcystin analysis by condensed phase membrane introduction tandem mass spectrometry. Anal. Methods https://doi.org/10.1039/c8ay00516h.

Falconer, I.R., 1991. Tumor promotion and liver injury caused by oral consumption of cyanobacteria. Environ. Toxicol. Water Qual. https://doi.org/10.1002/tox.2530060207.

Fayad, P.B., Roy-Lachapelle, A., Duy, S.V., Sauvé, S., 2015. On-line solid-phase extraction coupled to liquid chromatography tandem mass spectrometry for the analysis of cyanotoxins in algal blooms. Toxicon https://doi.org/10.1016/j.toxicon.2015.10.010.

Flores, N.M., Miller, T.R., Stockwell, J.D., 2018. A global analysis of the relationship between concentrations of microcystins in water and fish. Front. Mar. Sci. https://doi.org/10.3389/fmars.2018.00030.

Foss, A.J., Aubel, M.T., 2015. Using the MMPB technique to confirm microcystin concentrations in water measured by ELISA and HPLC (UV, MS, MS/MS). Toxicon https://doi.org/10.1016/j.toxicon.2015.07.332.

Foss, A.J., Butt, J., Fuller, S., Cieslik, K., Aubel, M.T., Wertz, T., 2017. Nodularin from benthic freshwater periphyton and implications for trophic transfer. Toxicon https://doi.org/10.1016/j.toxicon.2017.10.023.

Geis-Asteggiante, L., Lehotay, S.J., Fortis, L.L., Paoli, G., Wijey, C., Heinzen, H., 2011. Development and validation of a rapid method for microcystins in fish and comparing LC-MS/MS results with ELISA. Anal. Bioanal. Chem. https://doi.org/10.1007/s00216-011-5345-0.

Gene, S.M., Shahmohamadloo, R.S., Ortiz, X., Prosser, R.S., 2019. Effect of Microcystis aeruginosa–associated microcystin-LR on the survival of 2 life stages of freshwater mussel (Lampsilis siliquoidea). Environ. Toxicol. Chem. https://doi.org/10.1002/etc.4527.

Greer, B., Maul, R., Campbell, K., Elliott, C.T., 2017. Detection of freshwater cyanotoxins and measurement of masked microcystins in tilapia from Southeast Asian aquaculture farms. Anal. Bioanal. Chem. https://doi.org/10.1007/s00216-017-0352-4.

Greer, B., Meneely, J.P., Elliott, C.T., 2018. Uptake and accumulation of Microcystin-LR based on exposure through drinking water: an animal model assessing the human health risk. Sci. Rep. https://doi.org/10.1038/s41598-018-23312-7.

Huisman, J., Codd, G.A., Paerl, H.W., Ibelings, B.W., Verspagen, J.M.H., Visser, P.M., 2018. Cyanobacterial blooms. Nat. Rev. Microbiol. https://doi.org/10.1038/s41579-018-0040-1.

Humbert, J.F., 2009. Toxins of cyanobacteria. Handbook of Toxicology of Chemical Warfare Agents. https://doi.org/10.1016/B978-012374484-5.00027-4.

Kubickova, B., Babica, P., Hilscherová, K., Šindlerová, L., 2019. Effects of cyanobacterial toxins on the human gastrointestinal tract and the mucosal innate immune system. Environ. Sci. Eur. https://doi.org/10.1186/s12302-019-0212-2.

Lawrence, J.F., Menard, C., 2001. Determination of microcystins in blue-green algae, fish and water using liquid chromatography with ultraviolet detection after sample clean-up employing immunoaffinity chromatography. J. Chromatogr. A https://doi.org/10.1016/S0021-9673(01)00924-4.

Lemieux, R.U., Rudloff, E. Von, 1955. Periodate–permanganate oxidations: I. Oxidation of olefins. Can. J. Chem. https://doi.org/10.1139/v55-208.

Lemiuex, R.U., Rudloff, E. von, 1955. Periodate-permanganate oxidations. Can. J. Chem. 33 (11), 1701–1709.

Martens, S., 2017. Handbook of cyanobacterial monitoring and cyanotoxin analysis. Adv. Oceanogr. Limnol. https://doi.org/10.4081/aiol.2017.7221.

McLellan, N.L., Manderville, R.A., 2017. Toxic mechanisms of microcystins in mammals. Toxicol. Res. https://doi.org/10.1039/c7tx00043j.

Mekebri, A., Blondina, G.J., Crane, D.B., 2009. Method validation of microcystins in water and tissue by enhanced liquid chromatography tandem mass spectrometry. J. Chromatogr. A https://doi.org/10.1016/j.chroma.2009.01.095.

Metcalf, J.S., Bell, S.G., Codd, G.A., 2000. Production of novel polyclonal antibodies against the cyanobacterial toxin microcystin-LR and their application for the detection and quantification of microcystins and nodularin. Water Res. https://doi.org/10.1016/S0043-1354(99)00429-7.

Mohamed, Z., Ahmed, Z., Bakr, A., Hashem, M., Alamri, S., 2019. Detection of free and bound microcystins in tilapia fish from Egyptian fishpond farms and its related public health risk assessment. J. fur Verbraucherschutz und Leb. https://doi.org/10.1007/s00003-019-01254-0.

Moreno, I.M., Herrador, M.Á., Atencio, L., Puerto, M., González, A.G., Cameán, A.M., 2011. Differentiation between microcystin contaminated and uncontaminated fish by determination of unconjugated MCs using an ELISA anti-adda test based on receiver-operating characteristic curves threshold values: application to Tinca tinca from natural ponds. Environ. Toxicol. https://doi.org/10.1002/tox.20528.

Nagata, S., Soutome, H., Tsutsumi, T., Hasegawa, A., Sekijima, M., Sugamata, M., Harada, K.-I., Suganuma, M., Ueno, Y., 1995. Novel monoclonal antibodies against microcystin and their protective activity for hepatotoxicity. Nat. Toxins https://doi.org/10.1002/nt.2620030204.

Neffling, M.R., Lance, E., Meriluoto, J., 2010. Detection of free and covalently bound microcystins in animal tissues by liquid chromatography-tandem mass spectrometry. Environ. Pollut. https://doi.org/10.1016/j.envpol.2009.10.023.

Ortiz, X., Carabellido, L., Martí, M., Martí, R., Tomás, X., Díaz-Ferrero, J., 2011. Elimination of persistent organic pollutants from fish oil with solid adsorbents. Chemosphere https://doi.org/10.1016/j.chemosphere.2010.12.017.

Ortiz, X., Korenkova, E., Jobst, K.J., MacPherson, K.A., Reiner, E.J., 2017. A high throughput targeted and non-targeted method for the analysis of microcystins and anatoxin-A using on-line solid phase extraction coupled to liquid chromatography–quadrupole time-of-flight high resolution mass spectrometry. Anal. Bioanal. Chem. 409, 4959–4969. https://doi.org/10.1007/s00216-017-0437-0.

Ott, J.L., Carmichael, W.W., 2006. LC/ESI/MS method development for the analysis of hepatotoxic cyclic peptide microcystins in animal tissues. Toxicon https://doi.org/10.1016/j.toxicon.2006.01.025.

Plackett, R.L., Burman, J.P., 2006. The design of optimum multifactorial experiments. Biometrika https://doi.org/10.2307/2332195.

Rinehart, K.L., Harada, K.I., Namikoshi, M., Chen, C., Harvis, C.A., Munro, M.H.G., Blunt, J.W., Mulligan, P.E., Beasley, V.R., Dahlem, A.M., Carmichael, W.W., 1988. Nodularin, microcystin, and the configuration of Adda. J. Am. Chem. Soc. https://doi.org/10.1021/ja00233a049.

Robinson, N.A., Matson, C.F., Pace, J.G., 1991. Association of microcystin-LR and its biotransformation product with a hepatic-cytosolic protein. J. Biochem. Toxicol. https://doi.org/10.1002/jbt.2570060303.

Roy-Lachapelle, A., Fayad, P.B., Sinotte, M., Deblois, C., Sauvé, S., 2014. Total microcystins analysis in water using laser diode thermal desorption-atmospheric pressure chemical ionization-tandem mass spectrometry. Anal. Chim. Acta https://doi.org/10.1016/j.aca.2014.02.021.

Roy-Lachapelle, A., Solliec, M., Sinotte, M., Deblois, C., Sauvé, S., 2015. Total analysis of microcystins in fish tissue using laser thermal desorption-atmospheric pressure chemical ionization-high-resolution mass spectrometry (LDTD-APCI-HRMS). J. Agric. Food Chem. https://doi.org/10.1021/acs.jafc.5b02318.

Schmidt, J.R., Shaskus, M., Estenik, J.F., Oesch, C., Khidekel, R., Boyer, G.L., 2013. Variations in the microcystin content of different fish species collected from a Eutrophic Lake. Toxins (Basel) https://doi.org/10.3390/toxins5050992.

Shahmohamadloo, R.S., Ortiz Almirall, X., Holeton, C., Chong-Kit, R., Poirier, D.G., Bhavsar, S.P., Sibley, P.K., 2019a. An efficient and affordable laboratory method to produce and sustain high concentrations of microcystins by Microcystis aeruginosa. MethodsX https://doi.org/10.1016/j.mex.2019.10.024.

Shahmohamadloo, R.S., Poirier, D.G., Ortiz Almirall, X., Bhavsar, S.P., Sibley, P.K., 2019b. Assessing the toxicity of cell-bound microcystins on freshwater pelagic and benthic invertebrates. Ecotoxicol. Environ. Saf. https://doi.org/10.1016/j.ecoenv.2019.109945.

Shahmohamadloo, R.S., Simmons, D.B., Sibley, P.K., 2020. Shotgun proteomics analysis reveals sub-lethal effects in Daphnia magna exposed to cell-bound microcystins produced by Microcystis aeruginosa. Comp. Biochem. Phys. D. https://doi.org/10.1016/j.cbd.2020.100656.

Suchy, P., Berry, J., 2012. Detection of total microcystin in fish tissues based on lemieux oxidation and recovery of 2-methyl-3-methoxy-4-phenylbutanoic acid (MMPB) by solid-phase microextraction gas chromatography-mass spectrometry (SPME-GC/MS). Int. J. Environ. Anal. Chem. https://doi.org/10.1080/03067319.2011.620703.

Svirčev, Z., Lalić, D., Savić, G.B., Tokodi, N., Backović, D.D., Chen, L., Meriluoto, J., Codd, G.A., 2019. Global geographical and historical overview of cyanotoxin distribution and cyanobacterial poisonings. Arch. Toxicol. https://doi.org/10.1007/s00204-019-02524-4.

Vudathala, D., Smith, S., Khoo, L., Kuhn, D.D., Mainous, M.E., Steadman, J., Murphy, L., 2017. Analysis of microcystin-LR and nodularin using triple quad liquid chromatography-tandem mass spectrometry and histopathology in experimental fish. Toxicon https://doi.org/10.1016/j.toxicon.2017.08.005.

Ward, C.J., Beattie, K.A., Lee, E.Y.C., Codd, G.A., 1997. Colorimetric protein phosphatase inhibition assay of laboratory strains and natural blooms of cyanobacteria: comparisons with high-performance liquid chromatographic analysis for microcystins. FEMS Microbiol. Lett. https://doi.org/10.1016/S0378-1097(97)00290-5.

WHO, 2008. Guidelines for Drinking-Water Quality. Inc. 1st 2nd Addenda. 3rd ed. https://doi.org/10.1016/S1462-0758(00)00006-6 Geneva.

Wituszynski, D.M., Hu, C., Zhang, F., Chaffin, J.D., Lee, J., Ludsin, S.A., Martin, J.F., 2017. Microcystin in Lake Erie fish: risk to human health and relationship to

cyanobacterial blooms. J. Great Lakes Res. https://doi.org/10.1016/j.jglr.2017.08.006.

Wu, X., Xiao, B., Li, R., Wang, Z., Chen, Xiaoguo, Chen, Xudong, 2009. Rapid quantification of total microcystins in cyanobacterial samples by periodate-permanganate oxidation and reversed-phase liquid chromatography. Anal. Chim. Acta https://doi.org/10.1016/j.aca.2009.08.026.

Žegura, B., Gajski, G., Štraser, A., Garaj-Vrhovac, V., Filipič, M., 2011. Microcystin-LR induced DNA damage in human peripheral blood lymphocytes. Mutat. Res. - Genet. Toxicol. Environ. Mutagen. https://doi.org/10.1016/j.mrgentox.2011.10.002.